Environmental Science and Pollution Research (2023) 30:47501–47515
https://doi.org/10.1007/s11356-023-25667-5

RESEARCH ARTICLE

The evolution of ecological security and its drivers in the Yellow River Basin

Guolong Zhang[1] · Jianping Huang[1,2] · Xiaoyue Liu[2] · Xiaodan Guan[1,2] · Yun Wei[2] · Lei Ding[2] · Dongliang Han[1]

Received: 15 September 2022 / Accepted: 28 January 2023 / Published online: 6 February 2023

Abstract

Ecological security is the state achieved once an ecosystem maintains its stability under external stress. The Yellow River Basin (YRB) is the largest river basin in northwest and north China and an important area for grain and energy production. The assessment and attribution of ecological security in the YRB are important for protecting the natural environment and ensuring sustainable development. Here, the ecological security of the YRB was assessed by the ecological security index (ESI), a comprehensive index based on the oxygen cycle, and its drivers were attributed to climate change, human activities, vegetation, and soil factors. The spatial pattern of ecological security in the YRB showed high heterogeneity. Ecological insecurity occurred mainly in the middle reaches and regions where the major stream of the Yellow River passes through. The ESI decreased at a rate of − 0.82/year since 2000, which indicated the natural environment continued to be improved in the YRB. Climate change dominated the evolution of ecological security in the upper reaches. The level of ecological security has been improved in the middle reaches after a series of ecological restoration projects conducted. With higher intensity of industrial activity, human activities played a more critical role in ecological security in the lower reaches. Our results suggested that government and local people need to adopt different strategies and actions based on the dominant drivers in the upper, middle, and lower reaches to ensure protection of the natural environment and achieve sustainable development targets.

Keywords Ecological security · Oxygen cycle · Yellow River Basin · Climate change · Human activities

Introduction

Ecological security refers to a state in which natural and semi-natural ecosystems can maintain their stability and provides a guarantee of the sustainability of the eco-economic system (Rapport 1989; IUCN 2012; Liu and Chang 2015). With economic development, rapid industrialization, and urbanization, human activities have generated increasing pressure on the natural environment, which has disturbed the aquatic environment and habitats, decreased terrestrial diversity, and destroyed ecosystem functions (Chu et al. 2017; Yang et al. 2018). As the largest developing country in the world, China has experienced rapid economic development and accelerated urbanization since the reform and opening up, and ecological security has been threatened.

The YRB is an important base of grain and energy production in China and plays a vitally important role in the maintenance of China's ecological security (Wang et al. 2017). Climate change has significantly influenced ecological security in the YRB in recent decades. The increasing temperature has led to permafrost thawing and grassland degradation in the headstream region. Severe soil erosion due to the dry climate and complex topography threatened the conservation of water and soil in the middle reaches (Xiao et al. 2021). The decreasing precipitation and increasing population have increased the risk of water insecurity in the middle and lower reaches (Jia et al. 2015; Ringler et al. 2010). Due to the dense cities, large population, and fragile ecological environment, the ecological environment impact resulting from human activities is particularly significant in the YRB. During the past 100 years, the basin's population has more than increased from 50 to 190 million, whereas

Responsible Editor: Thomas Hein

✉ Jianping Huang
hjp@lzu.edu.cn

[1] Collaborative Innovation Center for Western Ecological Safety, Lanzhou University, Lanzhou 730000, China

[2] Key Laboratory for Semi-Arid Climate Change of the Ministry of Education, College of Atmospheric Sciences, Lanzhou University, Lanzhou 730000, China

urbanization rates doubled from 18 to 40% between 1980 and 2006 (Wohlfart et al. 2016). To increase agricultural production, the irrigated area expanded from increased from 800,000 ha in 1950 to 7,500,000 ha today, which resulted in the decreasing runoff of the Yellow River since the 1950s (Chen et al. 2020a). There is an urgent need to realize the coordinated development of social development and ecological security, and then promote the high-quality development of the YRB. A series of ecological restoration projects in China, especially the large-scale policy-driven Grain to Green Program, which has the aim of returning cultivated land to forest, was implemented in 2000 in the middle reaches of the YRB (Li 2004; Fu et al. 2017; Wu et al. 2019; Yin et al. 2021). Although ecological restoration programs have promoted the restoration of forest and grassland, the fragility of the ecosystems has still constrained the supply of ecosystem services and the social economic development in the YRB (Jia et al. 2022). Since 2019, ecological protection and high-quality development in the YRB have been promoted as a national strategy, marking a new historical period for local ecological environment and social development (Chen et al. 2020b). Therefore, to protect the natural environment and achieve sustainable development targets, there is an urgent need to assess the ecological security evolution of the YRB under the background of increased human activities and climate changes and clarify the main drivers of ecological security in the YRB.

However, the assessment of ecological security is difficult due to the complex interactions between social and ecological systems. Among many previous studies, several methods have been proposed to assess ecological security, such as the pressure–state–response model (Zhao et al. 2006; Wang et al. 2019), mathematical methods such as the gray model (Chen and Wang 2020) and fuzzy comprehensive evaluation method (Onkal-Engin et al. 2004), ecological methods such as the ecological service model (Huang et al. 2017) and ecological footprint model (Huang et al. 2007; Li et al. 2019; Yang et al. 2018), landscape ecological model (Yu et al. 2018; Xu et al. 2016), and geographic information system (Feng et al. 2018; Xie et al. 2020). The pressure–state–response model is the most widely used method; however, it usually provides a static assessment and cannot reflect the interactions of different factors and the evolution of ecological security.

Oxygen is a critically important gas for life on earth, and changes in its concentration are directly and closely related to human health, biological extinction, and ecological security (Huang et al. 2021; Jane et al. 2021). As the long-term declines in oxygen concentrations in lakes, oceans, and atmospheric linked to climate warming and enhanced human activity, the ecosystem function has been destroyed (Li et al. 2020; Jane et al. 2021), and ecological security has been severely threatened (Palmer et al. 2004; Huang et al. 2012, 2016, 2020a; Feng et al. 2018). The oxygen cycle is closely associated with the biological, carbon, hydrological, and thermal cycles. Since the oxygen budget was assessed by Huang et al. (2018), the oxygen cycle has been widely used to assess the ecological status of global cities, land, and oceans (Li et al. 2020, 2021; Han et al. 2021), and those indicators have proven to be a powerful tool to assess the ecological status of land and cities at the global scale (Huang et al. 2020a; Wei et al. 2021). Huang et al. (2020a) evaluated the global land ecological security covering the past 60 years and projected the oxygen balance with climate change for the future 100 years. Wei et al. (2021) investigated the oxygen balance and its related risks in 391 global large cities using the oxygen index and found that the oxygen index can be used to help assess and promote urban sustainability at broad scales. However, the effectiveness of an ecological security assessment based on the oxygen cycle over a local region, such as a river basin, has not yet been determined.

In this study, we addressed the following questions: (1) How did ecological security evolve based on the oxygen cycle in the YRB? (2) What are the main drivers that have influenced ecological security in the YRB during the last 3 decades? The rest of this paper is organized as follows: the "Datasets and methods" section briefly describes the general situation of the study area as well as data collection and processing, and then the methods used in this paper are introduced. The "Results" section gives the main results of this study. We discussed the ability of the ESI and the drivers of ecological security in YRB in the "Discussion" section. The main conclusions were drawn in the "Conclusion" section.

Datasets and methods

In this study, the ecological security is identified by the ecological security index (ESI), which was constructed by oxygen consumption (O_c), oxygen production (O_p), temperature warming magnification (T_m), and aridity index (AI), the drivers of which including climate change, human activities, vegetation, land use, and soil properties. The data compilation and method are described below.

Study region

The YRB covers four geomorphic units from west to east, namely, the Qinghai–Tibet Plateau, the Inner Mongolia Plateau, the Loess Plateau, and the Huang–Huaihai Plain (32–42°N, 96–119°E). The altitude of the YRB decreases from the west to the east, with a topographic difference of 3000 m (Xiao et al. 2021). Following previous studies (Lin et al. 2020; Zhang et al. 2022), we divided the YRB

into three sub-regions: upper reaches (Qinghai, Inner Mongolia, Ningxia, Gansu, and Sichuan), middle reaches (Shaanxi and Shanxi), and lower reaches (Shandong and Henan) in this study (Fig. 1a). The annual total precipitation of the entire basin is 466 mm, showing a decreasing pattern from southeast to west. The mean annual temperature ranges from – 4 to 14 °C (Ma et al. 2018). The grassland covers the most region of the upper reaches, most tree of YRB is located in the middle reaches, and cropland was found in the middle and lower reaches (Fig. 1b).

Datasets

Multiple datasets were collected from different sources as follows (Table 1), and illustrations of the data and procedural steps of the study are shown in Fig. 2.

The oxygen datasets

In these studies, we followed Huang et al. (2020a) to combine the balance between oxygen consumption with production, T_m, and AI to indicate the ecological security statute in the YRB, which was defined as

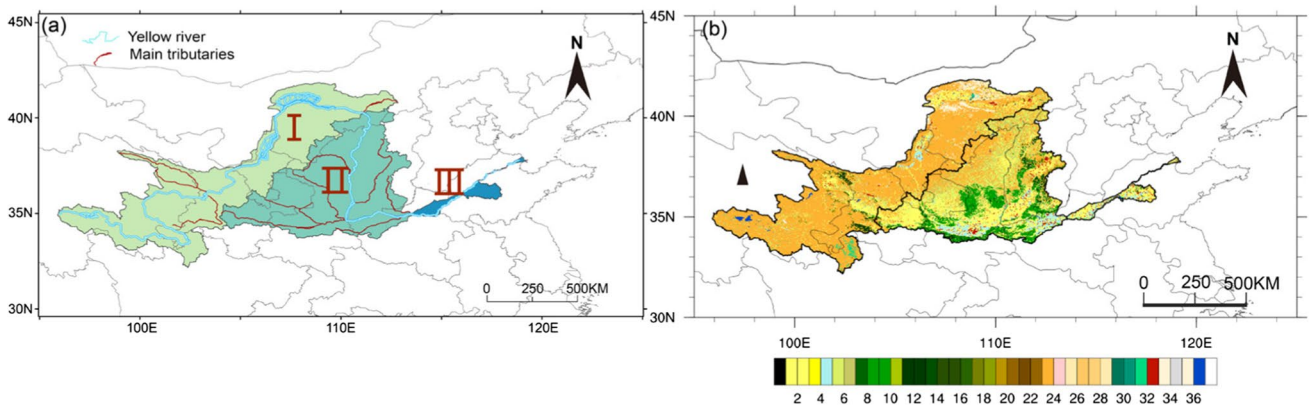

Fig. 1 The location (**a**) of the upper (I), middle (II), and lower reaches (III) and land cover (**b**) in the Yellow River Basin (1–4: cropland; 5–6: mosaic cropland/natural vegetation; 7–17: tree cover; 18–19: mosaic tree and shrub; 20–22: shrubland; 23: grassland; 24: lichens and mosses; 25–28: sparse vegetation; 29–30: tree cover; 32: urban; 33–35: bare area; 36: water body; 37: permanent snow and ice)

Table 1 The datasets and sources used in this study

No	Datasets	Data description	Data source	Use
1	Oxygen datasets	Oxygen consumption datasets	Huang et al. (2018) and Liu et al. (2020)	ESI calculation
		Net ecosystem productivity, heterotrophic, and soil respiration datasets	Global fire emissions database	
2	Land datasets	soil organic carbon	Global soil organic carbon map	ESI attribution
		Cropland datasets	Yu et al. (2021)	
		Terrace datasets	Cao et al. (2021)	
3	Socioeconomic datasets	Gross domestic product and human development Index datasets	Kummu et al. (2018)	ESI attribution
4	Vegetation datasets	Leaf area index datasets	http://www.glass.umd.edu/Download.html	ESI attribution
		Vegetation optical depth datasets	Moesinger et al. (2020)	LAI validation
5	Climate and hydrography datasets	Runoff datasets	Abatzoglou et al. (2018)	ESI validation
		Precipitation datasets	Climatic Prediction Center	AI calculation
		Potential evaporation datasets	CRU TS 3.25 dataset	
		Temperature warming magnification datasets	Huang et al. (2017)	ESI calculation
6	GDVI datasets	Global desertification vulnerability index datasets	Huang et al. (2020b)	ESI validation

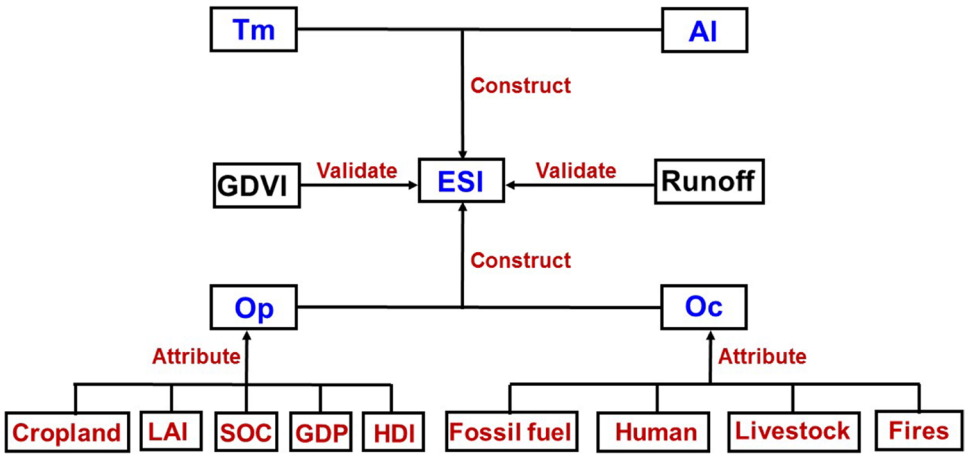

Fig. 2 Illustration of the overall methodology and procedural steps of the study. Here, ESI: ecological security index; Op: oxygen production; Oc: oxygen consumption; Tm: temperature warming magnification; AI: aridity index; GDVI: global desertification index; cropland: area fraction of cropland; LAI: leaf area index; SOC: soil organic carbon; GDP: gross domestic product; HDI: human development index

$$\mathrm{ESI} = \left(\frac{O_c}{O_p} * T_m * \frac{1}{\mathrm{AI}}\right)^{1/3} * 10 \tag{1}$$

O_c is the oxygen consumption consumed by four main processes, including (1) fossil fuel combustion, (2) human respiration, (3) livestock respiration, and (4) fires (Petsch 2014). The detailed methods and datasets of the processes could be found in previous studies (Huang et al. 2018; Liu et al. 2020).

O_p is the oxygen production that is produced during photosynthesis, during which plants and other organisms absorb carbon dioxide (CO_2) from the atmosphere and release oxygen (O_2). Photosynthesis can be expressed by the following chemical equation:

$$6H_2O + 6CO_2 \rightarrow C_6H_{12}O_6 + 6O_2 \tag{2}$$

According to Eq. (2), we can use Eq. (3) to calculate the net amount of O_2 produced during the process of photosynthesis if the known amount of carbon is fixed through photosynthesis (NEP). More detail could be found in Huang et al. (2018).

$$O_p = \mathrm{NEP} \times 2.667 \tag{3}$$

Here, NEP is the net amount of gross primary productivity (NPP) remaining after excluding the cost of plant and soil respiration (Rh), which is calculated by the following equation:

$$\mathrm{NEP} = \mathrm{NPP} - \mathrm{Rh} \tag{4}$$

The observed NPP, heterotrophic, and soil respiration from 2000 to 2015 were acquired from the Global Fire Emissions Database (van der Werf et al. 2017).

T_m is the temperature warming magnification, which is defined as the ratio of the grid warming rate to the global warming rate as follows:

$$T_m(i,n) = \frac{T_{\mathrm{trend}}(i,n)}{T_{\mathrm{Gtrend}(n)}} \tag{5}$$

where $T_{\mathrm{trend}}(i,n)$ is defined as the linear trend of the surface temperature from 1901 to year n at grid point i, and $T_{\mathrm{Gtrend}}(n)$ is defined as the linear trend of the global average surface temperature from 1901 to year n for year n (Huang et al. 2017).

Climate and Hydrography Datasets

The AI was widely used to indicate the aridity state of the atmosphere, which is defined as the ratio of precipitation to potential evapotranspiration (PET):

$$\mathrm{AI} = \frac{P}{\mathrm{PET}} \tag{6}$$

Here, the precipitation data provided by the Climatic Prediction Center (CPC) cover 1948 to the present with a spatial resolution of 30 arc-seconds. The PET data is from CRU TS 3.25 dataset (Harris et al. 2014), which covers the period 1901–2016 and all land areas at 0.5° resolution. The runoff data with high-spatial resolution (1/24°) from 1958 to 2015 was provided by Abatzoglou et al. (2018), who produced monthly surface water balance datasets using a water balance model that incorporates reference evapotranspiration, precipitation, temperature, and interpolated plant extractable soil water capacity.

Vegetation datasets

The LAI and VOD data were retrieved from satellite observation. The satellite-observed LAI products (GIMMS LAI) derived from the Advanced Very High-Resolution Radiometer are currently considered the best dataset for overcoming

data inconsistencies resulting from the utilization of multiple satellite sensor systems (Zhu et al. 2013). The VOD data derived from multiple space-borne microwave sensors were produced by Moesinger et al. (2020) using the land parameter retrieval model. There are the Ku-band (period 1987–2017), X-band (1997–2018), and C-band (2002–2018) data, the spatial resolution of which is 30 arc-seconds. In this study, the Ku-band data was used due to the long time records.

Land datasets

The soil organic carbon was extracted from the global soil organic carbon map, which is the first global soil organic carbon map ever produced through a consultative and participatory process involving member countries, which makes this map totally new and unique (http://www.fao.org/soils-portal/data-hub/soil-maps-and-databases/global-soil-organic-carbon-map-gsocmap/en/). The terrace data was extracted time-series spectral features and topographic features from Landsat 8 images and the shuttle radar topography mission digital elevation model data, classifying cropland area into terraced and non-terraced types through a random forest classifier (Cao et al. 2021). The cropland data was retrieved from a continuously covered cropland distribution dataset in China spanning from 1900 to 2016 by assimilating multiple data sources (Yu et al. 2021).

Socioeconomic data

As the population data was used to calculate the oxygen consumption, here, gross domestic product (GDP) and human development index (HDI) were used to indicate the level of human economic and social development. HDI is a composite index of 'average achievement in key dimensions of human development: [i] a long and healthy life, [ii] being knowledgeable, and [iii] having a decent standard of living (UNDP 2017). Both the GDP and HDI were retrieved from Kummu et al. (2018), who reproduced annual global gridded datasets at 5 arc-min resolution for the 25-year period of 1990–2014.

As different spatial resolutions of datasets, we interpolated the data to a resolution of $0.1 \times 0.1°$. Additionally, some of the data sets had a different time length; 2000–2015 was chosen to calculate the mean of variables.

Statistical methods

Linear regression analysis

The trends of O_c, O_p, LAI, VOD, and HDI were calculated as the slope of linear regression using the ordinary method:

$$\text{Slope} = \frac{n * \sum_{i=1}^{n}(i * A_i) - \sum_{i=1}^{n} i * \sum_{i=1}^{n} A_i}{n * \sum_{i=1}^{n} i^2 - (\sum_{i=1}^{n} i)^2} \quad (7)$$

where n was the length of time series, i was the number of year, and A_i was O_c, O_p, HDI, and environmental factors in the *ith* year.

Multivariate adaptive regression splines method

The multivariate adaptive regression splines (Jerome 1991; MARS) were used to attribute the spatial patterns in oxygen production to vegetation, human activities, and soil/land changes. MARS is a nonparametric regression method based on pricewise linear regressions, which does not assume a distribution between the response and predictor variables. In this study, the MARS models were computed with R package earth (https://cran.r-project.org/web/packages/earth/index.html) and were construed for upper, middle, and lower reaches, respectively.

Result

The evolution of ecological security in the YRB

As shown in Fig. 3a, the oxygen consumption was high in the lower reaches and low in the upper reaches. There was a high-value center of oxygen consumption located in the Fenhe–Weihe Basin. The more intense the human activities, the higher the oxygen consumption and the greater the risk of natural environmental insecurity. Oxygen production decreased from south to north in the YRB. The region with the largest oxygen production was located in the southeastern Gansu Province and in the south-central region of Shanxi Province (Fig. 3b). The regions with the lowest oxygen production were located in the upper reaches (Fig. 3b). Due to high spatial heterogeneity in oxygen consumption and production and rapid climate change, the ESI showed high spatial heterogeneity in the YRB (Fig. 4). The higher the ESI value, the greater the insecurity of environment. The ESI value decreased from east to west, indicating that the level of ecological security increased from east to west in the YRB. Ecological insecurity occurred mainly in the regions through which the mainstream of the Yellow River passed, such as the Yinchuan Plain and western Hetao Plain. The regions with the highest level of ecological security were mainly located in the southern Gansu Province and eastern Qinghai Province. Figure 4c shows that ESI values decreased at the speed of 0.82/year from 2000 to 2014, indicating that ecological security has significantly improved in the YRB.

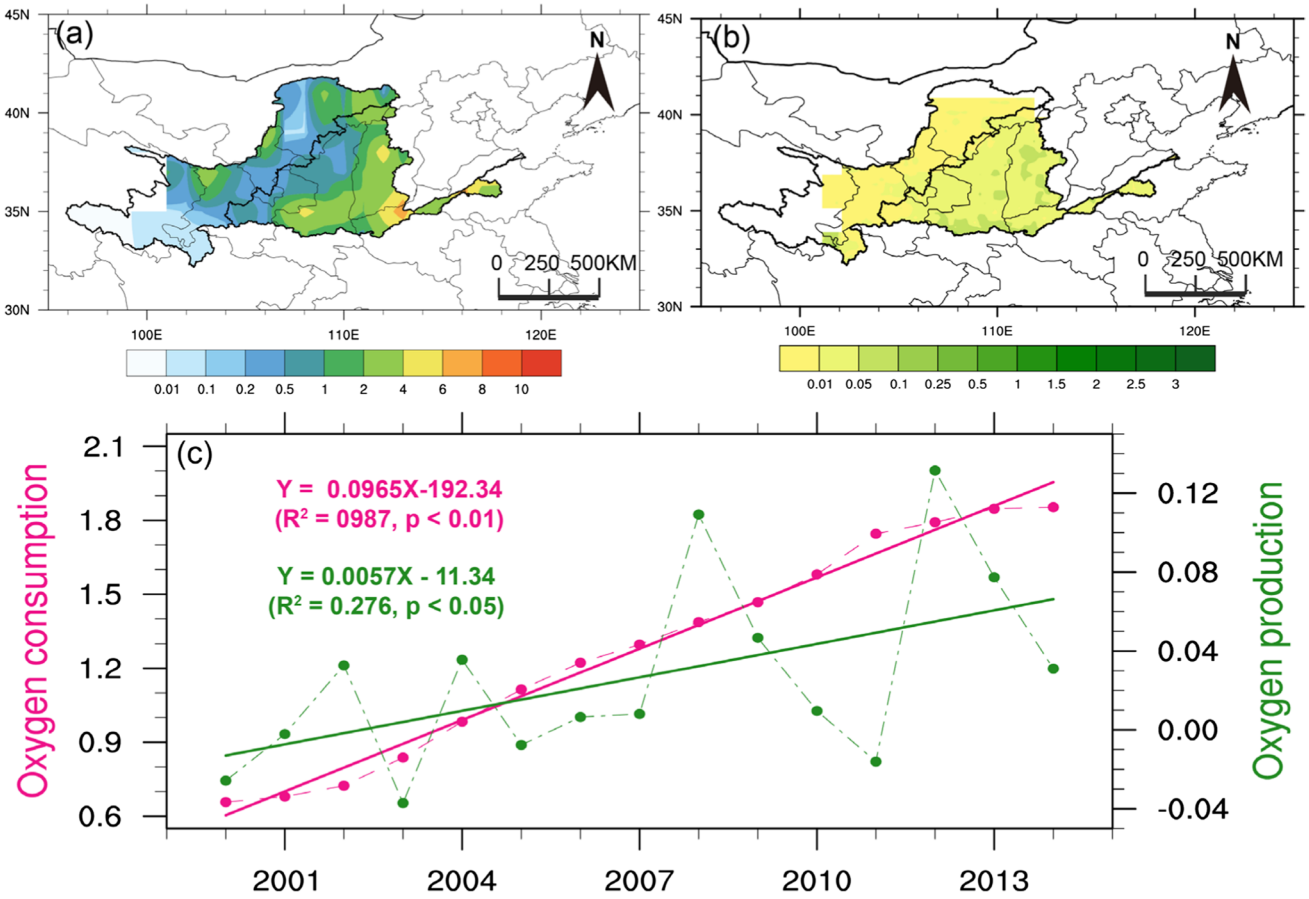

Fig. 3 The average distributions of oxygen consumption (**a**), oxygen production (**b**) during 2000–2014, and evolution (**c**) in the Yellow River Basin. The forest green line and deep pink line indicate the oxygen production and oxygen consumption in (c), respectively

Most regions of the YRB are in arid, semi-arid, or semi-humid climate zones, and the YRB also suffers from the risk of desertification, which also is an important issue for the local environment. We assessed the risk of desertification based on the global desertification vulnerability index (GDVI) (Huang et al. 2020b), which is used to assess the desertification risk due to climate change and human activities. The higher the GDVI value, the more severe the desertification risk. The GDVI indicated high desertification risk in the upper reaches (Fig. 4b). The regions with high desertification risk were located along the borders of Gansu Province, Ningxia Province, and Inner Mongolia Autonomous Region, which are surrounded by the Tengger Desert, Badain Jaran Desert, and Kubuqi Desert (Fig. 4b), where the level of the ecological security is also low. Due to the wet climate and dense vegetation cover, the level of ecological security was high and the desertification risk was low in the southern middle reaches. Both the desertification risk has decreased and the ecological security has improved during past decades (Fig. 4c), indicating the ecological and environmental improvements in the YRB.

Drivers of change in ecological security

The pattern of ecological security in the YRB was influenced by climate change and human activities. With human activities and economic development, oxygen was consumed. The process of oxygen production was also influenced by human activities such as city, cropland expansion, and deforestation. Soil characters are important for plant growth and soil respiration, and LAI is the direct factor affecting the speed of photosynthesis and influences the NEP. Both soil and vegetation character influence the vulnerability of the ecosystem. Climate change can change the growing conditions for vegetation and impact the local environment. Therefore, we attributed the land ecological security changes to climate change, soil and vegetation change, and human activities in this study. The evolutions of these factors are as follows.

Climate change

Under global warming, the temperature increased in all basins during the past 3 decades (Mao et al. 2018). The

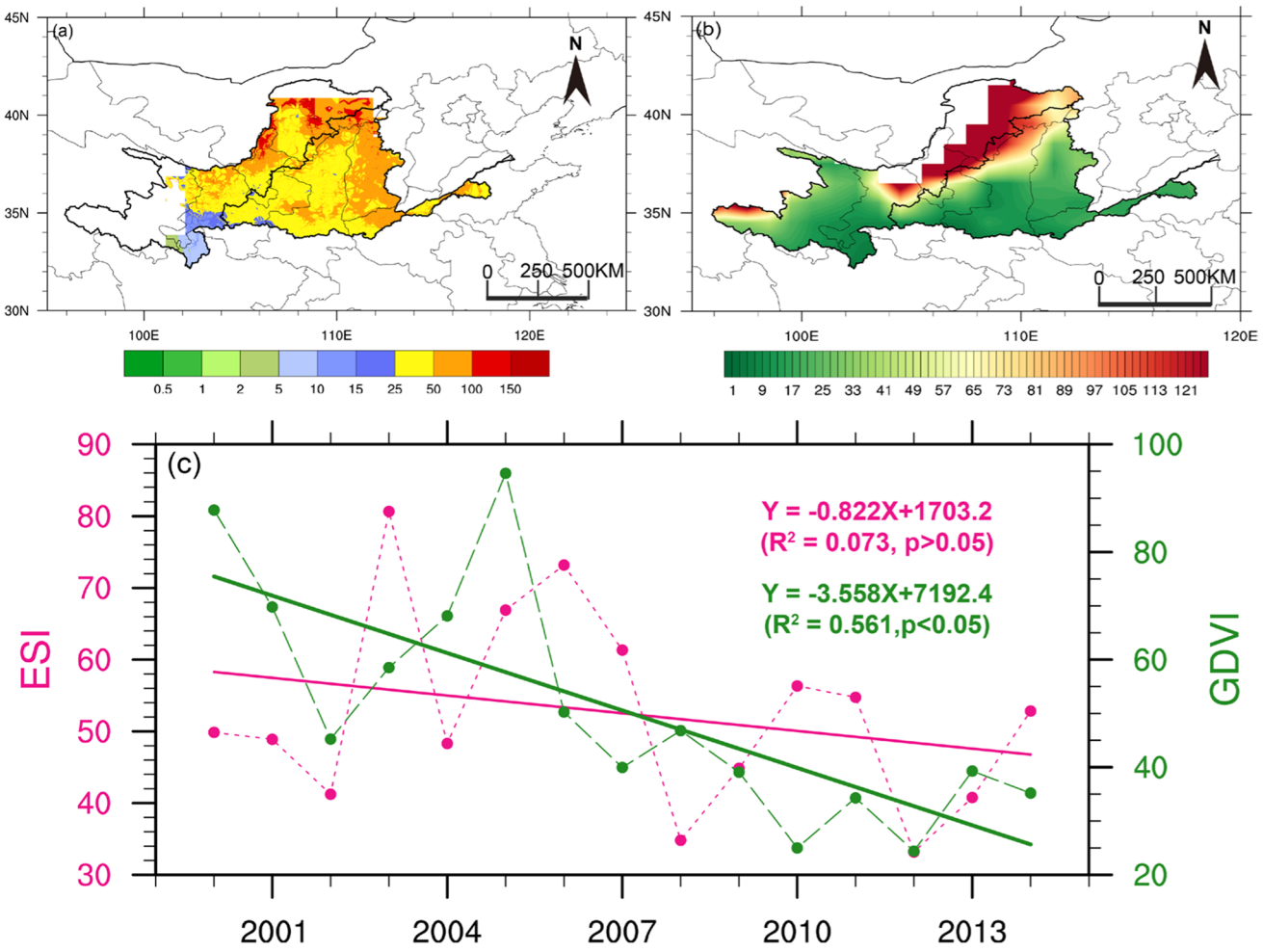

Fig. 4 The average distributions of ecological security index (ESI) (**a**), desertification vulnerability index (GDVI) (**b**) during 2000–2014, and evolution (**c**) in the Yellow River Basin. The forest green line and deep pink line indicate the GDVI and ESI in (c), respectively

regions with the fastest temperature increase were located in the headstream of the YRB and eastern Hetao Plain (Fig. 5a). In contrast to the consistently increasing temperature pattern, the distribution of precipitation change in the YRB displayed high spatial heterogeneity. Precipitation increased in the headstream and part of the region in the Hetao Plain. The largest decreasing precipitation was observed in the southern part of the middle reaches (Fig. 5b), which may be the main factor responsible for the decreasing runoff in the middle and lower reaches. Most regions of the YRB are arid, semi-arid, and semi-humid climate zones, with the AI increasing from west to east and from north to south (Fig. 5c). The AI increased after 2000 in the YRB, indicating that the basin became wetter, while it increased strongly in the upper reaches due to increasing precipitation (Fig. 5d).

Vegetation

Figure 6 shows the spatial distribution of vegetation cover in the YRB. In general, the vegetation cover was generally high in the southern basin but low in the northern basin. The highest LAI values were found in the southern middle reaches, followed by the southwest of Gansu Province (Fig. 6a). The LAI showed an increasing trend in the upper, middle, and lower reaches, with the largest rate of increase in the middle reaches, followed by the lower and upper reaches (Fig. 6b). The LAI suddenly increased since 2000 in the upper and middle reaches, which may due to the implementation of the Grain to Green large-scale revegetation program since 1999. The spatial distribution of VOD was similar to the pattern of the LAI, with high values located in the southern YRB. Compared with the LAI, the rate of increase of

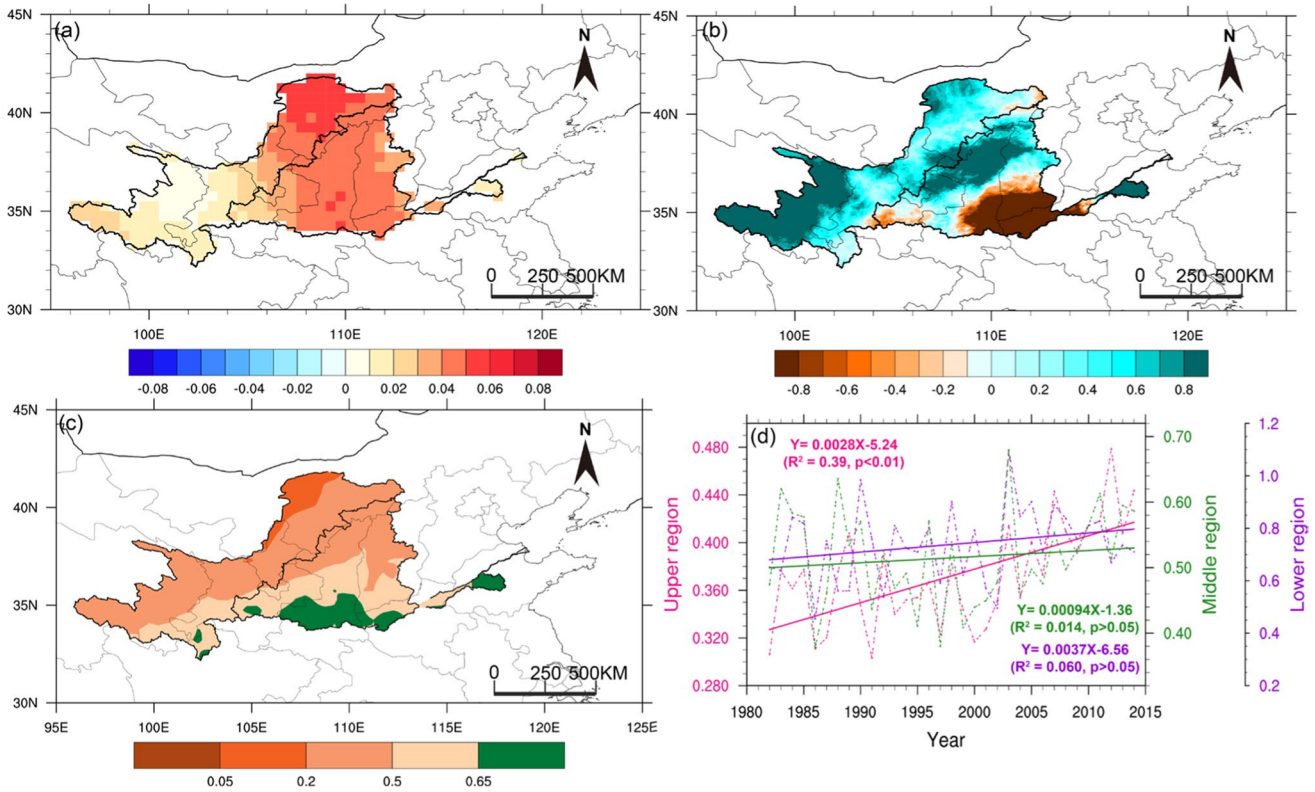

Fig. 5 Climate change in the Yellow River Basin. The distribution of trends in temperature (**a**) and precipitation (**b**) during 1982–2014; the average distributions of annual the aridity index (AI, **c**) during 1982–2014; the evolution of the AI in the upper (deep pink line), middle (forest green line), and lower reaches (dark violet line) (d)

VOD was larger in each of the upper, middle, and lower reaches (Fig. 6c). The VOD increased rapidly from 2000 to 2008 but slowed down after 2008 in the lower and middle reaches (Fig. 6d). The VOD increased rapidly from 2000 to 2014 in the upper reaches, with no slowing downtrend after 2008.

Land characters

The soil organic carbon content was high in the headstream of the YRB and the region where the Grain to Green large-scale revegetation program was implemented (Fig. 7a). This result indicates that the revegetation program has significantly improved the soil quality of the Loess Plateau. The high organic carbon content in the headstream implies that the area has an important ecosystem function and that it is necessary to protect ecosystems to achieve the carbon peak target. Most of the river terraces were located in the middle reaches of the YRB (Fig. 7b), which was mainly a consequence of the specific local topography. The distribution of river terraces was similar to that of the decreased runoff in the YRB, which indicated a strong influence of human activities on the ecosystem in the middle reaches.

Cropland is an important indicator of land use change. Figure 8 shows the distribution of cropland in the YRB. Most cropland was located in the middle and lower reaches. The cropland distribution was similar to the spatial distribution of GDP (Fig. 8), which had high-value centers located in the Guanzhong Plain and along the mainstream Yellow River. The area fraction of cropland decreased significantly from 20.5% in 2000 to 19.2% in 2014. The most significant period of decrease was in approximately 2000, which was when the Grain to Green program was conducted. The decrease in cropland directly reflected the efforts to promote public awareness regarding environmental protection and ecological conservation in the YRB.

Human activities

GDP indicates the level of economic development and reflects the direct pressure of human activities on the environment. As Fig. 9 shows, there was a high value of GDP in regions with urban agglomerations, such as Lanzhou and Xi'an city, which are provincial capital cities. The low value of GDP indicated the relatively low level of human activities in the upper reaches. Compared with the upper reaches, the

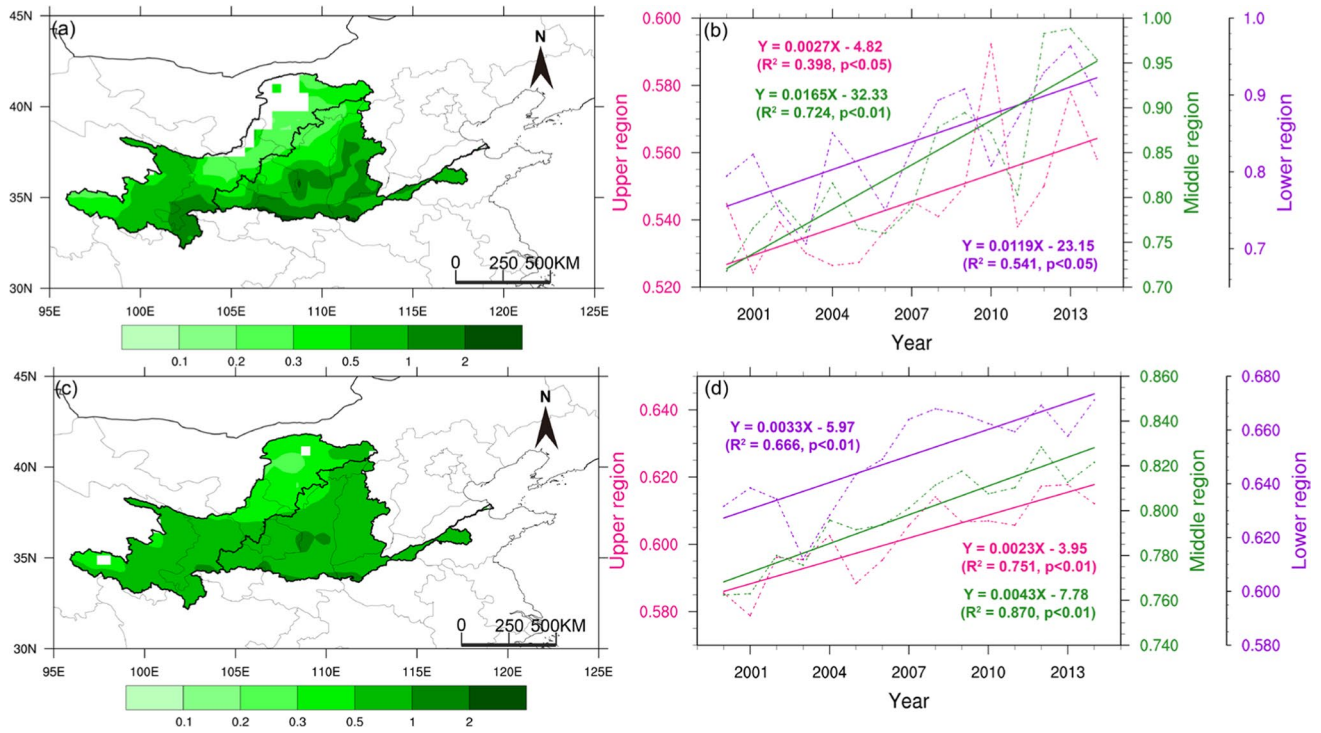

Fig. 6 Changes in vegetation parameters in the Yellow River Basin. The average distributions of the leaf area index (LAI, **a**) and vegetation optical depth (VOD, **c**) during 2000–2014 and the evolution of LAI (**b**) and VOD (**d**). The deep pink line represents the upper reaches, the forest green line the middle reaches, and the dark violet line the lower reaches in (b) and (d)

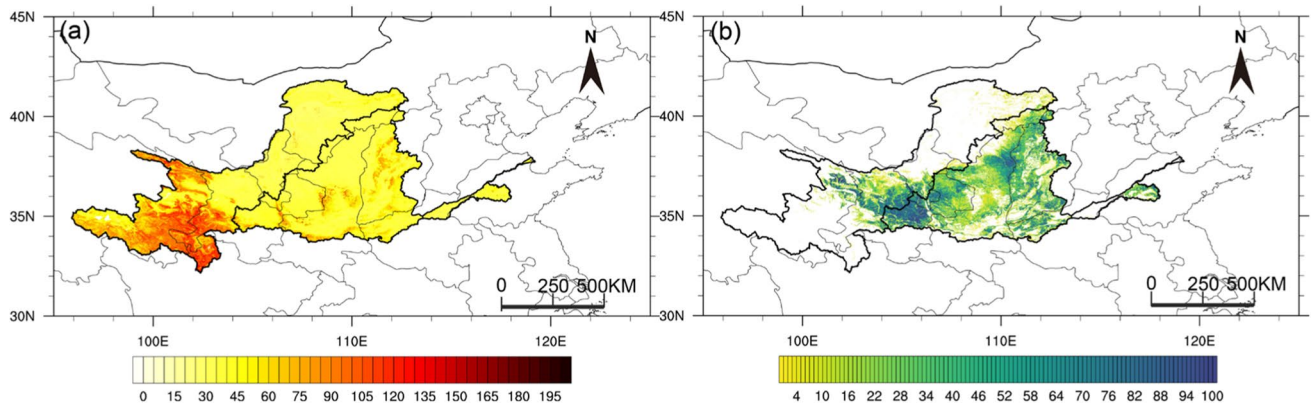

Fig. 7 The average distributions of soil organic carbon (SOC, **a**) and terraces (**b**) in the Yellow River Basin during 2000–2014

value of GDP was larger in the lower and middle reaches. There was a belt with a high value of GDP that ran from the northwest to the southeast in the middle reaches. The spatial pattern of GDP was similar to the distribution of ecological security, which indicated a strong impact of human activities on the local natural environment in the middle and lower reaches.

The HDI increased from west to east in the YRB, which was in line with economic development and education. The upper reaches had a low HDI, while regions with a high HDI were located in Shandong Province and the Inner Mongolia Autonomous Region (Fig. 9b). The HDI increased from 0.57 to 0.72 during 2000–2014, and the GDP increased exponentially (Fig. 9c), indicating that the economy developed and population increased in the YRB during this period. Although the spatial resolution of the HDI was 5 arc-min, the HDI in the provincial administrative regions remained constant, which may be due to the raw data source only providing information at the provincial level.

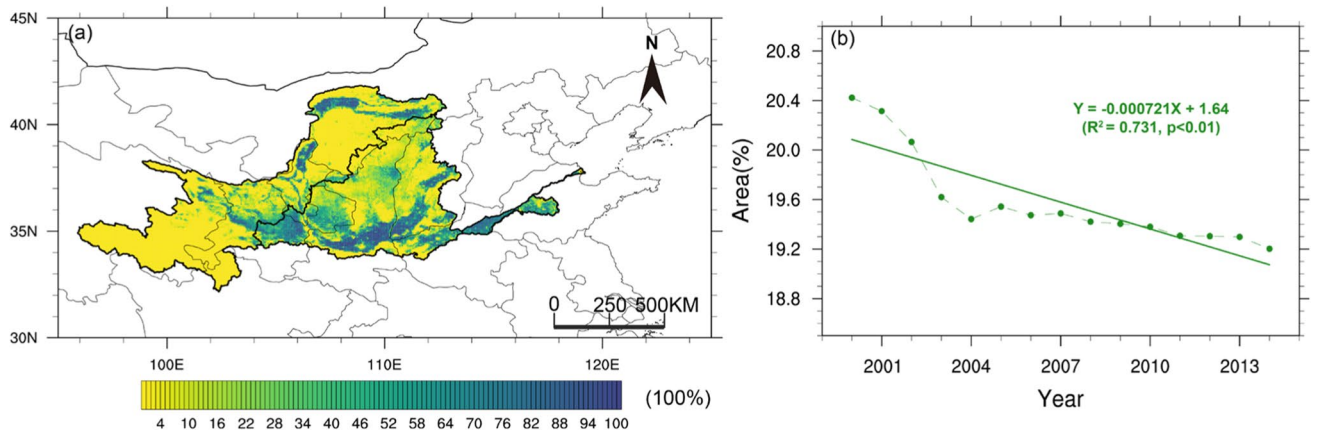

Fig. 8 Changes in the cropland area fraction in the Yellow River Basin during 2000–2014. The average distribution of cropland area fraction during 2000–2014 (**a**) and a time series of the cropland area fraction (**b**)

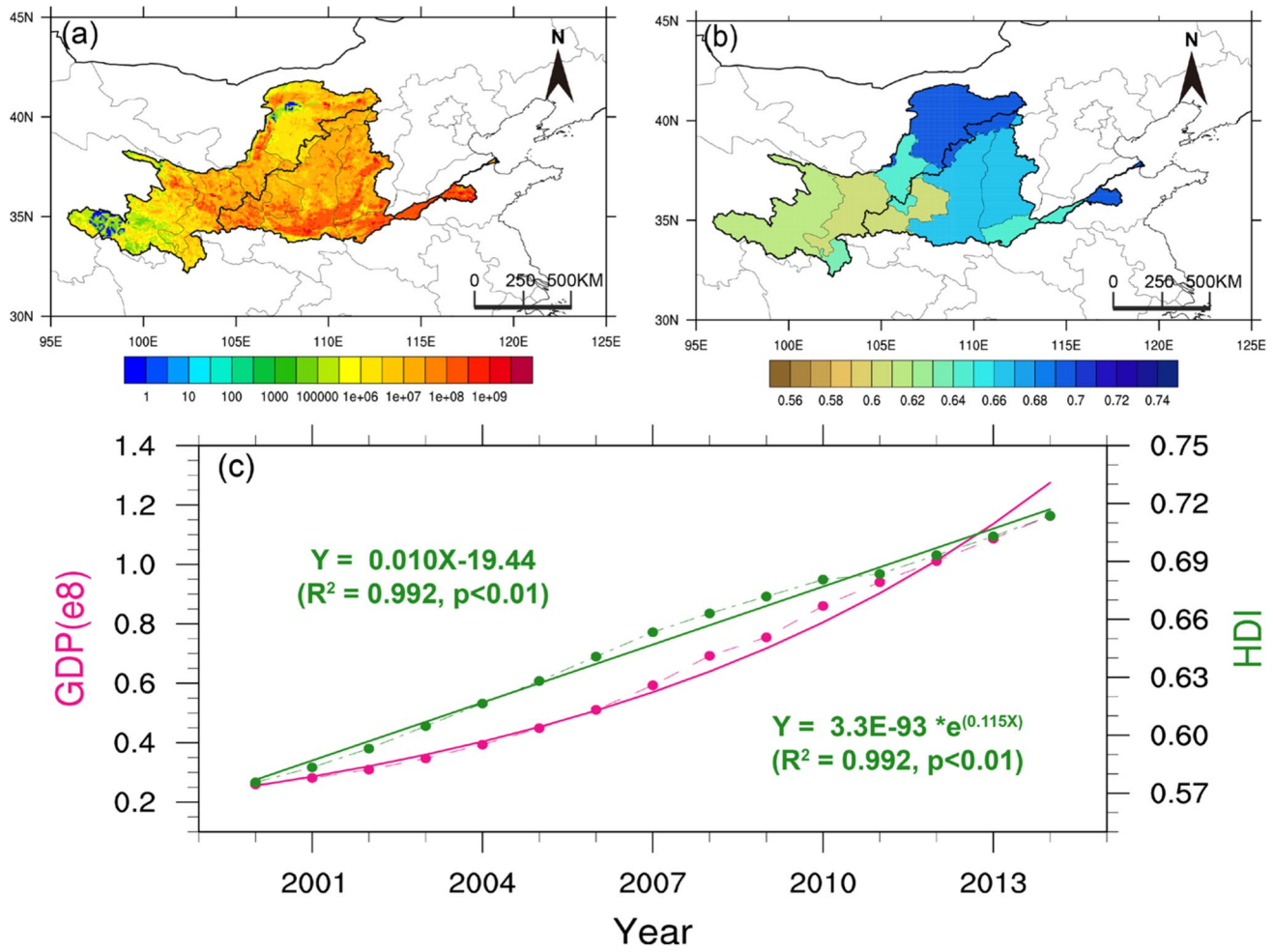

Fig. 9 Changes in the gross domestic product (GDP) and human development index (HDI) in the Yellow River Basin during 2000–2014. The average distributions of GDP (**a**) and HDI (**b**) during 2000–2014 and their time series (**c**) in the Yellow River Basin. The forest green line and deep pink line indicate the GDP and HDI in (c), respectively

Discussion

The reliability of the ESI

As oxygen is the most important survival factor of all animals on the earth, the oxygen cycle is closely associated with biological, carbon, hydrological, and thermal cycles. ESI was proposed to diagnose and project a land ecological security-based oxygen cycle. Previous study showed that a severe decline in ecological security has occurred in drylands that have expanded into surrounding regions over the past 60 years, and the response of ecological security to global warming and human activities is projected to be stronger based on ESI (Huang et al. 2020a). Geoscientists can apply the newly proposed ESI to investigate and reanalyze the vitality of land with different ecological statuses and optimize the gains from the constructions of ecological civilization.

In this study, the ESI results indicated that the areas with threatened ecosystems were located in the region where the mainstream of the river passed through and in the lower reaches where high levels of human activity were indicated by GDP data. As most regions of the YRB are located in the arid, semi-arid, or semi-humid zones, water resources are the main constraint factor both for economic development and the environment, which is why most cities are located in the region where the mainstream of the river passed through. Previous studies showed that areas with high levels of economic development were located in the middle and lower reaches of the basin and were associated with high levels of urban expansion (Ji et al. 2021).

The ESI indicated improved ecological security since 2000, which is consistent with the results of previous research (Jiang et al. 2021; Zhao et al. 2021). Zhang et al. (2022) showed that the ecological vulnerability level shows a decreasing trend from 2001 to 2019 in the YRB, indicating the ecological environmental quality had improved in the YRB. A series of ecological restoration projects, such as the Three-north Shelterbelt, the Grain-for-Green, the Natural Forest Projection, and the Yellow River Basin Comprehensive Planning (2012–2030), were conducted in the YRB; the vegetation coverage increased and the ecological environment was improved (Li et al. 2016; Lv et al. 2019; Zhang et al. 2021).

Overall, the ESI could diagnose the spatial pattern and evolution of ecological security in the YRB. However, in regions where oxygen consumption is low due to a lack of human activities, it is difficult to reveal the potential ecological risk using the ESI. The ESI value was low in the upper reaches due to the limited human activity, while there was a high desertification risk due to the foliage ecosystem and increasing temperature. Previous studies also have shown that vegetation began to degenerate or experience more rapid degradation since 2007 due to permafrost degradation and overgrazing (Song et al. 2018). Water is critical to the local natural environment and to economic development (Wang et al. 2019). As shown in Fig. 10, the runoff distribution pattern was spatially heterogeneous, with large runoff volumes in the headstream, southern middle reaches, and lower reaches. In the Yinchuan Plain and western Hetao Plain, there were smaller volumes of runoff. The regional average runoff displayed a slightly increasing trend from 1982 to 2014. Due to the human activities in the major stream of the YRB, water security will be a bottleneck that restricts the development of the local social economy. By combining ESI and GDVI, we presented a comprehensive picture of the ecological security of the YRB.

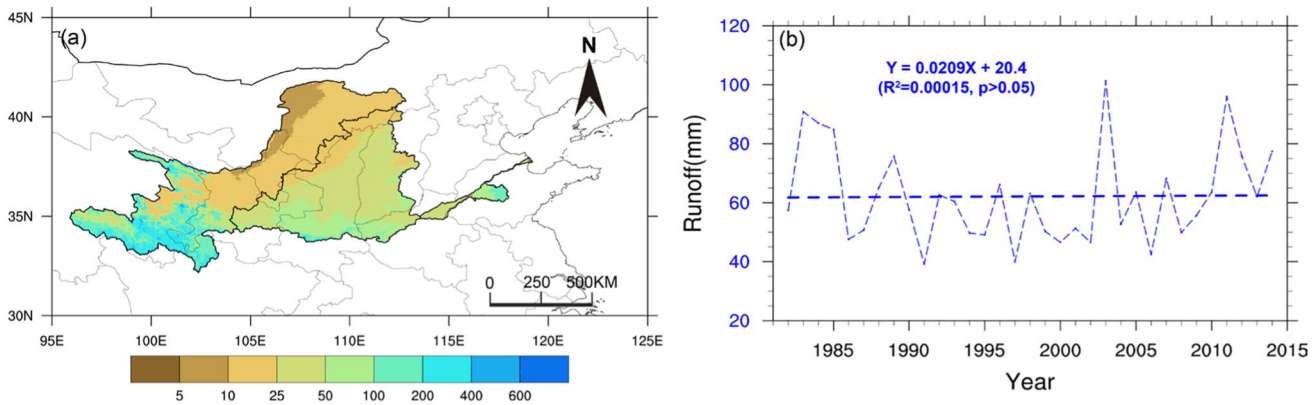

Fig. 10 Change in the volume of runoff in the Yellow River Basin during 1982–2014. The average distribution of annual total runoff during 1982–2014 (**a**) and a time series of the runoff (**b**) (unit: mm)

The influence of drivers in the upper, middle, and lower reaches

The ESI represents the oxygen balance between consumption and ecological support under climate change. Due to the different industrial structures and climatological environments, the dominant factors of oxygen consumption and production were different. It is very important to clarify the dominant factors of oxygen consumption and production in the upper, middle, and lower reaches.

Oxygen consumption was dominated by fossil fuel combustion in the upper, middle, and lower reaches. Most of the fossil fuel combustion occurred in the middle reaches due to the intense industrial activity (Fig. 11a), which is an important factor impacting local ecological security. That is due to the rich coal, natural gas, oil, and nonferrous metal resources in the middle reach (Liu et al. 2021). Population and livestock were also important factors that affected the oxygen consumption in the lower reaches, while there was little fossil fuel compared with the upper and middle reaches. In the lower reaches, with a high level of economic development, there are prone to form population agglomeration zones, implying a high demand for water and pressure on the local environment. Following fossil fuel combustion, livestock was the next largest consumer of oxygen in the upper reaches. As previous studies showed that grazing is an important factor in grassland degradation (Xu et al. 2017; Shi et al. 2020).

The multivariate adaptive regression revealed that the LAI dominated the oxygen production pattern in the middle and lower reaches because the vegetation is the direct source of oxygen production. The increasing LAI in the lower reaches was due to more effective cropland management, leading to increased crop production (Chen et al. 2019). The LAI and VOD significantly increased (Fig. 5b, 5d), which was closely associated with government policy in the middle reaches. The HDI was the main factor influencing the pattern of oxygen production in the upper reaches, followed by the LAI, area of cropland, GDP, and soil organic carbon content. HDI is closely related to the level of human education and awareness of environmental protection. A higher HDI has a positive impact on the local environment, and a lower HDI may accompany the destructive activities to the local environment, which influences oxygen production. In the upper reaches, the vegetation is sparse and oxygen production is small, the human activities would have a significant influence on the local environment and oxygen production, which is why the HDI dominated the oxygen production in the upper reaches. The increasing HDI had an effective influence on improving ecological security in the YRB. With the increasing temperature in the upper reaches (Fig. 4a), the lengthened vegetation growing season was an important factor that increased the annual LAI and VOD in the upper reaches; however, it was also accompanied by the thawing of permafrost, the amount of carbon released into the atmosphere increased (Fig. 6a), which will accelerate the speed of warming and cancel the positive effect of increasing temperature in the future.

In summary, with government policy, a wetter climate (Fig. 5d), and increased vegetation coverage, oxygen

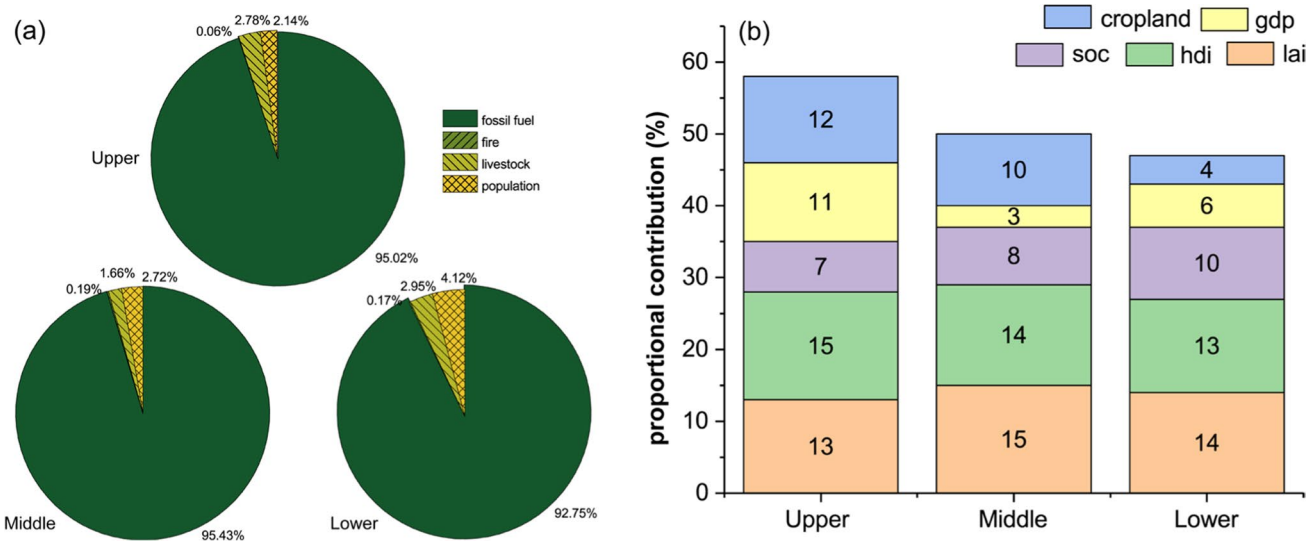

Fig. 11 Attribution of oxygen changes in the upper, middle, and lower reaches. The contribution of different factors to oxygen consumption; the areas show the proportional contribution of each driver (**a**). The proportional contribution of different factors to oxygen production using multivariate adaptive regression; the bars show the importance (measured as the percentage of the overall variance explained) of individual drivers (**b**). The drivers are LAI (leaf area index), GDP (gross domestic production), HDI (human development index), cropland (area of cropland), and SOC (soil organic carbon)

production has significantly increased, and the level of ecological security has been improved in the past three decades in the YRB (Fig. 3). It is noted that we qualitatively investigated the driver of ecological security in the YRB by analyzing dominated factor of oxygen consumption and production and the effect of climate change on the local environment in this study. The quantitative contribution was not given; that should be fatherly investigated in future studies.

Conclusion

Achieving sustainable development goals requires a balance to be maintained between the environment, society, and the economy. Environmental sustainability has always been an important part of sustainable development and is a necessary condition for achieving strong overall sustainability. To achieve environmental sustainability, a reasonable index can guide policymakers in the right direction. We combined oxygen consumption, oxygen production, global warming, and the extent of land aridity to construct the ESI to assess the ecological security of the YRB. The ESI decreased at a rate of − 0.82/year since 2000, which indicated that the natural environment continued to be improved in the YRB. ESI could present the spatial pattern of ecological security in the YRB: the higher ecological insecurity is located in the middle reaches and mainstream of the Yellow River, with the largest oxygen imbalance. The highest desertification risk was located in the northwestern YRB. Due to the fragile environment, both human activities and climate change had an important effect on the evolution of ecological security in the upper reaches. As a series of ecological restoration projects conducted, the government has improved the level of ecological security in the middle reaches. With higher levels of industrial activity, human activities played a more critical role in ecological security in the lower reaches. In the future, when balancing local economic development and the goal of reaching a carbon peak, government and citizens should consider the ecological capacity of the region with regard to its fragile environment and high desertification risk in the upper reaches. In the severe oxygen imbalance region, there is a need to take actions, such as optimizing energy consumption structure, upgrading industries, and developing a green economy, to reduce oxygen consumption and CO_2 emissions.

Acknowledgements This work was jointly supported by the National Natural Science Foundation of China (42041004 and 41991231), the Youth Science and Technology Fund Project of Gansu (21JR7RA527 and 21JR7RA521), and the Fundamental Research Funds for the Central Universities (lzujbky-2021-kb12 and lzujbky-2021-63).

Author contribution All authors contributed to the study's conception and design. Material preparation, data collection, and analysis were performed by Guolong Zhang, Xiaoyue Liu, Yun Wei, and Lei Ding. The first draft of the manuscript was written by Guolong Zhang, and all authors commented on previous versions of the manuscript. All authors read and approved the final manuscript.

Data availability The datasets used or analyzed during the current study are available from the corresponding author (hjp@lzu.edu.cn) upon reasonable request.

Declarations

Ethics approval and consent to participate Not applicable.

Consent for publication Not applicable.

Conflict of interest The authors declare no competing interests.

References

Abatzoglou JT, Dobrowski SZ, Parks SA, Hegewisch KC (2018) TerraClimate, a high-resolution global dataset of monthly climate and climatic water balance from 1958–2015. Sci Data 5(1):170191. https://doi.org/10.1038/sdata.2017.191

Cao B, Yu L, Naipal V, Ciais P, Li W, Zhao Y, Wei E, Chen D, Liu Z, Gong P (2021) A 30 m terrace mapping in China using Landsat 8 imagery and digital elevation model based on the Google Earth Engine. Earth Syst Sci Data 13(5):2437–2456. https://doi.org/10.5194/essd-13-2437-2021

Chen Y, Wang J (2020) Ecological security early-warning in central Yunnan Province, China, based on the gray model. Ecol Indic 111:106000. https://doi.org/10.1016/j.ecolind.2019.106000

Chen Y, Zhu M, Lu J, Zhou Q, Ma W (2020a) Evaluation of ecological city and analysis of obstacle factors under the background of high-quality development: taking cities in the Yellow River Basin as examples. Ecol Indic 118:106771. https://doi.org/10.1016/j.ecolind.2020.106771

Chen C, Park T, Wang X, Piao S, Xu B, Chaturvedi RK, . . . Myneni RB (2019) China and India lead in greening of the world through land-use management. Nat Sustain 2(2): 122–129. https://doi.org/10.1038/s41893-019-0220-7

Chen Y, Fu B, Zhao Y, Wang K, Zhao M, Ma J, . . . Wang H (2020b) Sustainable development in the Yellow River Basin: issues and strategies. J Clean Prod 263 121223. https://doi.org/10.1016/j.jclepro.2020.121223

Chu X, Deng X, Jin G, Wang Z, Li Z (2017) Ecological security assessment based on ecological footprint approach in Beijing-Tianjin-Hebei region, China. Phys Chem Earth, Parts a/b/c 101:43–51. https://doi.org/10.1016/j.pce.2017.05.001

Feng Y, Yang Q, Tong X, Chen L (2018) Evaluating land ecological security and examining its relationships with driving factors using GIS and generalized additive model. Sci Total Environ 633:1469–1479. https://doi.org/10.1016/j.scitotenv.2018.03.272

Fu B, Wang S, Liu Y, Liu J, Liang W, Miao C (2017) Hydrogeomorphic ecosystem responses to natural and anthropogenic changes in the Loess Plateau of China. Annu Rev Earth Planet Sci 45(1):223–243. https://doi.org/10.1146/annurev-earth-063016-020552

Han D, Huang J, Ding L, Liu X, Li C, Yang F (2021) Oxygen footprint: an indicator of the anthropogenic ecosystem changes. Catena 206:105501. https://doi.org/10.1016/j.catena.2021.105501

Harris I, Jones PD, Osborn TJ, Lister DH (2014) Updated high-resolution grids of monthly climatic observations – the CRU TS3.10 dataset. Int J Climatol 34:623–642. https://doi.org/10.1002/joc.3711

Huang Q, Wang R, Ren Z, Li J, Zhang H (2007) Regional ecological security assessment based on long periods of ecological footprint

analysis. Resour Conserv Recycl 51(1):24–41. https://doi.org/10.1016/j.resconrec.2006.07.004
Huang J, Guan X, Ji F (2012) Enhanced cold-season warming in semi-arid regions. Atmos Chem Phys 12(12):5391–5398. https://doi.org/10.5194/acp-12-5391-2012
Huang J, Yu H, Guan X, Wang G, Guo R (2016) Accelerated dryland expansion under climate change. Nat Clim Chang 6(2):166–171. https://doi.org/10.1038/nclimate2837
Huang J, Yu H, Dai A, Wei Y, Kang L (2017) Drylands face potential threat under 2 °C global warming target. Nat Clim Chang 7(6):417–422. https://doi.org/10.1038/nclimate3275
Huang J, Huang J, Liu X, Li C, Ding L, Yu H (2018) The global oxygen budget and its future projection. Sci Bull 63(18):1180–1186. https://doi.org/10.1016/j.scib.2018.07.023
Huang J, Zhang G, Zhang Y, Guan X, Wei Y, Guo R (2020b) Global desertification vulnerability to climate change and human activities. Land Degrad Dev 31(11):1380–1391. https://doi.org/10.1002/ldr.3556
Huang J, Yu H, Han D, Zhang G, Wei Y, Huang J, . . . Ren Y (2020a) Declines in global ecological security under climate change. Ecol Indic 117 106651. https://doi.org/10.1016/j.ecolind.2020.106651
Huang J, Liu X, He Y, Shen S, Hou Z, Li S, . . . Huang J (2021) The oxygen cycle and a habitable earth. Sci China Earth Sci 64(4): 511–528. https://doi.org/10.1007/s11430-020-9747-1
IUCN (2012) IUCN (International Union for Conservation of Nature) red list categories and criteria: version 3.1. IUCN Bulletin
Jane SF, Hansen GJA, Kraemer BM, Leavitt PR, Mincer JL, North RL, . . . Rose KC (2021) Widespread deoxygenation of temperate lakes. Nature 594(7861): 66–70. https://doi.org/10.1038/s41586-021-03550-y
Jerome HF (1991) Multivariate adaptive regression splines. Ann Stat 19(1):1–67. https://doi.org/10.1214/aos/1176347963
Ji Q, Liang W, Fu B, Zhang W, Yan J, Lv Y, . . . Yang P (2021) Mapping land use/cover dynamics of the Yellow River Basin from 1986 to 2018 supported by google Earth Engine. Remote Sens 13(7): 1299. https://doi.org/10.3390/rs13071299
Jia X, Li C, Cai Y, Wang X, Sun L (2015) An improved method for integrated water security assessment in the Yellow River basin, China. Stoch Env Res Risk Assess 29(8):2213–2227. https://doi.org/10.1007/s00477-014-1012-2
Jia G, Hu W, Zhang B, Li G, Shen S, Gao Z, Li Y (2022) Assessing impacts of the Ecological Retreat project on water conservation in the Yellow River Basin. Sci Total Environ 828:154483. https://doi.org/10.1016/j.scitotenv.2022.154483
Jiang L, Liu Y, Wu S, Yang C (2021) Analyzing ecological environment change and associated driving factors in China based on NDVI time series data. Ecol Indic 129:107933. https://doi.org/10.1016/j.ecolind.2021.107933
Kummu M, Taka M, Guillaume JHA (2018) Gridded global datasets for gross domestic product and human development index over 1990–2015. Sci Data 5(1):180004. https://doi.org/10.1038/sdata.2018.4
Li W (2004) Degradation and restoration of forest ecosystems in China. For Ecol Manage 201(1):33–41. https://doi.org/10.1016/j.foreco.2004.06.010
Li S, Liang W, Fu B, Lv Y, Fu S, Wang S, Su H (2016) Vegetation changes in recent large-scale ecological restoration projects and subsequent impact on water resources in China's Loess Plateau. Sci Total Environ 569–570:1032–1039. https://doi.org/10.1016/j.scitotenv.2016.06.141
Li J, Chen Y, Xu C, Li Z (2019) Evaluation and analysis of ecological security in arid areas of Central Asia based on the emergy ecological footprint (EEF) model. J Clean Prod 235:664–677. https://doi.org/10.1016/j.jclepro.2019.07.005
Li C, Huang J, Ding L, Liu X, Yu H, Huang J (2020) Increasing escape of oxygen from oceans under climate change. Geophys Res Lett 47(11): e2019GL086345. https://doi.org/10.1029/2019GL086345
Li C, Huang J, Ding L, Liu X, Han D, Huang J (2021) Estimation of oceanic and land carbon sinks based on the most recent oxygen budget. Earth's Future 9 e2021EF002124. https://doi.org/10.1029/2021EF002124
Lin M, Biswas A, Bennett EM (2020) Socio-ecological determinants on spatio-temporal changes of groundwater in the Yellow River Basin, China. Sci Total Environ 731:138725. https://doi.org/10.1016/j.scitotenv.2020.138725
Liu D, Chang Q (2015) Ecological security research progress in China. Acta Ecol Sin 35(5):111–121. https://doi.org/10.1016/j.chnaes.2015.07.001
Liu X, Huang J, Huang J, Li C, Ding L, Meng W (2020) Estimation of gridded atmospheric oxygen consumption from 1975 to 2018. J Meteorol Res 34(3):646–658. https://doi.org/10.1007/s13351-020-9133-7
Liu K, Qiao Y, Shi T, Zhou Q (2021) Study on coupling coordination and spatiotemporal heterogeneity between economic development and ecological environment of cities along the Yellow River Basin. Environ Sci Pollut Res 28:6898–6912. https://doi.org/10.1007/s11356-020-11051-0
Lv M, Ma Z, Li M, Zheng Z (2019) Quantitative analysis of terrestrial water storage changes under the Grain for Green Program in the Yellow River Basin. J Geophys Res: Atmospheres 124:1336–1351. https://doi.org/10.1029/2018JD029113
Ma L, Xia H, Sun J, Wang H, Feng G, Qin F (2018) Spatial–temporal variability of hydrothermal climate conditions in the Yellow River Basin from 1957 to 2015. Atmosphere 9(11):433. https://doi.org/10.3390/atmos9110433
Mao J, Carlton A, Cohen RC, Brune WH, Brown SS, Wolfe GM, Jimenez JL, Pye HOT, Lee Ng N, Xu L, McNeill VF, Tsigaridis K, McDonald BC, Warneke C, Guenther A, Alvarado MJ, de Gouw J, Mickley LJ, Leibensperger EM, Mathur R, Nolte CG, Portmann RW, Unger N, Tosca M, Horowitz LW (2018) Southeast atmosphere studies: learning from model-observation syntheses. Atmos Chem Phys 18:2615–2651. https://doi.org/10.5194/acp-18-2615-2018
Moesinger L, Dorigo W, de Jeu R, van der Schalie R, Scanlon T, Teubner I, Forkel M (2020) The global long-term microwave Vegetation Optical Depth Climate Archive (VODCA). Earth Syst Sci Data 12(1):177–196. https://doi.org/10.5194/essd-12-177-2020
Onkal-Engin G, Demir I, Hiz H (2004) Assessment of urban air quality in Istanbul using fuzzy synthetic evaluation. Atmos Environ 38(23):3809–3815. https://doi.org/10.1016/j.atmosenv.2004.03.058
Palmer M, Bernhardt E, Chornesky E, Collins S, Dobson A, Duke C, . . . Turner M (2004) Ecology for a crowded planet. Science, 304(5675): 1251. https://doi.org/10.1126/science.1095780
Petsch ST (2014) The Global Oxygen Cycle. In: Holland HD, Turekian KK (eds) Treatise on geochemistry, 2nd edn. Elsevier, Oxford, pp 437–473. https://doi.org/10.1016/B978-0-08-095975-7.00811-1
Rapport DJ (1989) What constitutes ecosystem health? Perspect Biol Med 33:120–132. https://doi.org/10.1353/pbm.1990.0004
Ringler C, Cai X, Wang J, Ahmed A, Xue Y, Xu Z, . . . You L (2010) Yellow River basin: living with scarcity. Water Int 35(5): 681–701. https://doi.org/10.1080/02508060.2010.509857
Shi F, Liu S, Sun Y, An Y, Zhao S, Liu Y, Li M (2020) Ecological network construction of the heterogeneous agro-pastoral areas in the upper Yellow River basin. Agric Ecosyst Environ 302:107069. https://doi.org/10.1016/j.agee.2020.107069
Song Y, Jin L, Wang H (2018) Vegetation changes along the Qinghai-Tibet Plateau engineering corridor since 2000 induced by climate change and human activities. Remote Sens 10(1):95. https://doi.org/10.3390/rs10010095

UNDP (2017) Human development reports database (United Nations Development Programme)

Wang X, Zhang J, Shamsuddin S, Oyang R, Guan T, Xue J, Zhang X (2017) Impacts of climate variability and changes on domestic water use in the Yellow River Basin of China. Mitig Adapt Strat Glob Change 22(4):595–608. https://doi.org/10.1007/s11027-015-9689-1

Wang Y, Zhao W, Wang S, Feng X, Liu Y (2019) Yellow River water rebalanced by human regulation. Sci Rep 9(1):9707. https://doi.org/10.1038/s41598-019-46063-5

Wei Y, Wu J, Huang J, Liu X, Han D, An L, . . . Huang J (2021) Declining oxygen level as an emerging concern to global cities. Environ Sci Technol 55(12): 7808–7817. https://doi.org/10.1021/acs.est.1c00553

Werf GR van der, Randerson JT, Giglio L, Leeuwen TT van, Chen Y, Rogers BM, . . . Kasibhatla PS (2017) Global fire emissions estimates during 1997–2016. Earth Syst Sci Data 9(2): 697-720. https://doi.org/10.5194/essd-9-697-2017

Wohlfart C, Kuenzer C, Chen C, Liu G (2016) Social–ecological challenges in the Yellow River basin (China): a review. Environ Earth Sci 75(13):1066. https://doi.org/10.1007/s12665-016-5864-2

Wu X, Wang S, Fu B, Feng X, Chen Y (2019) Socio-ecological changes on the Loess Plateau of China after Grain to Green Program. Sci Total Environ 678:565–573. https://doi.org/10.1016/j.scitotenv.2019.05.022

Xiao Y, Guo B, Lu Y, Zhang R, Zhang D, . . . Wang Z (2021) Spatial–temporal evolution patterns of soil erosion in the Yellow River Basin from 1990 to 2015: impacts of natural factors and land use change. Geomat Nat Hazards Risk 12(1): 103–122. https://doi.org/10.1080/19475705.2020.1861112

Xie H, He Y, Choi Y, Chen Q, Cheng H (2020) Warning of negative effects of land-use changes on ecological security based on GIS. Sci Total Environ 704:135427. https://doi.org/10.1016/j.scitotenv.2019.135427

Xu C, Pu L, Zhu M, Li J, Chen X, Wang X, Xie X (2016) Ecological security and ecosystem services in response to land use change in the coastal area of Jiangsu, China. Sustainability 8(8):816. https://doi.org/10.3390/su8080816

Xu H, Wang X, Zhang X (2017) Impacts of climate change and human activities on the aboveground production in alpine grasslands: a case study of the source region of the Yellow River, China. Arab J Geosci 10:17. https://doi.org/10.1007/s12517-016-2801-3

Yang Q, Liu G, Hao Y, Coscieme L, Zhang J, Jiang N, . . . Giannetti BF (2018) Quantitative analysis of the dynamic changes of ecological security in the provinces of China through emergy-ecological footprint hybrid indicators. J Clean Prod 184 678–695. https://doi.org/10.1016/j.jclepro.2018.02.271

Yin L, Feng X, Fu B, Wang S, Wang X, Chen Y, . . . Hu J (2021) A coupled human-natural system analysis of water yield in the Yellow River basin, China. Sci Total Environ 762 143141. https://doi.org/10.1016/j.scitotenv.2020.143141

Yu D, Wang D, Li W, Liu S, Zhu Y, Wu W, Zhou Y (2018) Decreased landscape ecological security of peri-urban cultivated land following rapid urbanization: an impediment to sustainable agriculture. Sustainability 10(2):394. https://doi.org/10.3390/su10020394

Yu Z, Jin X, Miao L, Yang X (2021) A historical reconstruction of cropland in China from 1900 to 2016. Earth Syst Sci Data 13(7):3203–3218. https://doi.org/10.5194/essd-13-3203-2021

Zhang D, Zuo X, Zang C (2021) Assessment of future potential carbon sequestration and water consumption in the construction area of the Three-North Shelterbelt Programme in China. Agric For Meteorol 303:108377. https://doi.org/10.1016/j.agrformet.2021.108377

Zhang X, Liu K, Wang S, Wu T, Li X, Wang J, Wang D, Zhu H, Tan C, Ji Y (2022) Spatiotemporal evolution of ecological vulnerability in the Yellow River Basin under ecological restoration initiatives. Ecol Indic 135:108586. https://doi.org/10.1016/j.ecolind.2022.108586

Zhao Y, Zou X, Cheng H, Jia H, Wu Y, Wang G, . . . Gao S (2006) Assessing the ecological security of the Tibetan plateau: methodology and a case study for Lhaze County. J Environ Manag 80(2): 120–131. https://doi.org/10.1016/j.jenvman.2005.08.019

Zhao Y, Hou P, Jiang J, Zhai J, Chen Y, Wang Y, . . . Xu H (2021) Coordination study on ecological and economic coupling of the Yellow River Basin. Int J Environ Res Public Health 18(20). https://doi.org/10.3390/ijerph182010664

Zhu Z, Bi J, Pan Y, Ganguly S, Anav A, Xu L, . . . Myneni RB (2013) Global data sets of vegetation leaf area index (LAI)3g and fraction of photosynthetically active radiation (FPAR)3g derived from global inventory modeling and mapping studies (GIMMS) normalized difference vegetation index (NDVI3g) for the period 1981 to 2011. Remote Sens 5(2): 927–948. https://doi.org/10.3390/rs5020927